A Receiver structure for coherent reception of M-ary orthogonal spread spectrum acoustic communications at very low SNR in shallow water environments

Paul J. Gendron
Electrical and Computer Engineering Department,
University of Massachusetts Dartmouth
North Dartmouth, MA 02747
Email: pgendron@umassd.edu

Abstract—**A receiver structure is proposed for M-ary orthogonal spread spectrum signaling that is effective at very low signal to noise ratio and without the aid of pilot symbols. The receiver models the coherent multi-path arrival structure with a motion dilation compensation scheme that takes advantage of the estimated coherent acoustic response function. To accommodate the rapid time varying behavior of the acoustic channel that is induced by platform motion and boundary interactions a hierarchical Gaussian mixture model based adaptive filtering scheme is presented. The mixture assignment over delay-Doppler-beam is used to accurately capture the sparse coherent features of the arrival structure. The correlated path dilation processes attendant with at-depth motion through a waveguide with small angle spreads are estimated from the coherent acoustic response. The mixture model based estimator replaces conventional time recursive Kalman-like schemes for channel estimation and takes advantage of the entire data set to make efficient estimation of the channel response at each symboling instant. This estimate of the response serves to ameliorate the coherence degrading effects of bulk platform motion replacing conventional phase locked loops for symbol timing and time dilation compensation. This allows the receiver to perform coherent symbol decisions against the natural coherence of the acoustic waveguide. This receiver was tested in shallow water ocean environments in Buzzards Bay MA. Empirical bit error rates are demonstrated at very low SNRs for coherent and non-coherent symbold decisions. Tests were conducted at various spreading gains and bandwidths to achieve rates up to 130 bps at 2km with a demonstrated probability of bit error of less than 10^{-4} with 3 element combining at SNRs less than -20 dB.** **[This work is funded by the Naval Innovative Science and Engineering Basic and Applied Research Program at SSC-Pacific as well as the Office of Naval Research]**

I. Introduction

Reliable acoustic communications at very low signal to noise ratio (SNR) will serve as an enabling technology to extend the reach of underwater networks. In cases where that network serves primarily command and control functions such a technology has significant value. As autonomy and on-board signal processing are refined to extend the functionality of underwater unmanned vehicles (UUVs) and sensor nodes the communication demands of command, control [25] and navigation [8] become limiting constraints. More generally, a wide range of undersea missions depend on acoustic communications and networking protocols [19] to fulfill their objectives. From mine countermeasures [26] to sensor networks for tactical surveillance [18] acoustic signaling serves as a vital information link to undersea system assets. It is expected that underwater sensor networks will continue to be enabling technologies for environmental monitoring roles such as oceanographic data collection for ocean/climate model refinement as well as pollution monitoring and disaster prevention [19].

Shallow water acoustic communication throughput rates are fundamentally limited by three physical constraints: First and foremost the slow propagation speed of sound in water implies numerous deleterious effects. Propagating over typical water depths and ranges, low sound speed implies a multi-path arrival structure that is unknown at the receiver and changes spatially and temporally as the receiver moves. This acoustic response must be estimated in order to coherently reconstruct the sent message. Secondly, platform and surface motion are not negligible relative to the slow speed of sound leading to Doppler spreading [22]. Together these constitute a doubly spread channel function whose accuracy of estimation is limited regardless of the duration of the message packet. In addition to these effects there is the significant latency of communications associated with slow propagation speeds [19]. Thirdly and just as critically the volume attenuation of sound in sea water is a strong function of frequency implying that bit throughput rates, proportional to channel bandwidth, are limited by propagation range [28]. In short, slow propagation phase velocity and frequency dependent volume attenuation for undersea acoustic propagation implies a far more challenging media than electro-magnetic free-space propagation does on terrestrial wireless links.

Underwater surveillance and monitoring missions typically require intermittent communications and for this reason coherent channel conditions are not known at the information source prior to signaling. An additional subtle feature that has significant effects on underwater acoustic communications is the channel's sparsity. The platform motion scenario, the structure of the waveguide, its refractive features, the water depth and range as well as bottom features all determine the multipath-Doppler spread character of the response function over the signaling interval. These features typically occupy a subspace of the delay-frequency-Doppler product of the channel. Underwater acoustic channels are typically sparse with an arrival structure that is not known a-priori.

Proposed here is a means of communicating at very low

978-0-933957-40-4 ©2013 MTS

This is a DRAFT. As such it may not be cited in other works. The citable Proceedings of the Conference will be published in IEEE Xplore shortly after the conclusion of the conference.

signal to noise ratio (SNR) at rates that can exceed the rates allowable in conventional direct-sequence spread spectrum schemes employing bpsk by a factor of 2 or more. The aim of this approach is to provide an enabling technology to underwater networks that must transmit payloads of information intermittently over exceptionally long distances or at low source power levels. The method is offered to significantly extend the coverage area of surveillance assets in scenarios where intermittent command and control communications dominate the media access requirements of the network. The approach, like all spread spectrum methods, trades bandwidth to achieve a requisite SNR per bit. The M-ary signaling scheme and the receiver proposed have the added advantage of allowing for coherent estimation of the channel response function over the entire time-bandwidth of the message without knowledge of the symbols sent or the reservation of time-bandwidth to pilot symbols of any kind.

The channel estimation approach offers a practical and conceptual alternative to applications of the Gauss-Markov model and Kalman-like approaches [14] [24] [13] [21]. Kalman-like algorithms fundamentally leverage the temporal coherence of the Green's function through appropriate averaging to ensure that the resulting estimates are statistically efficient. One shortcoming of these algorithms is that they are typically employed in a look-back framework, only exploiting preceding observations to make inferences regarding the present time sample. By marching forward in time and leveraging a Markov assumption regarding the process, these algorithms exploit a temporal model of the dynamics of the response process to make an estimate of the present state. This article develops and demonstrates an estimation scheme based on a mixture-Gaussian model over time/Doppler, frequency/selectivity and beam/angle such that the Green's function at any instant can be estimated given all of the data over the entire duration and bandwidth of the signal [9]. The resulting mixture-Gaussian framework allows for a level of flexibility in the regularization that is not as easily accomplished with Gauss-Markov models short of full forward-backward recursions.

II. A HIERARCHICAL MIXTURE MODEL FOR SPACE TIME VARYING ACOUSTIC RESPONSE FUNCTIONS

A. Review of the Ocean Acoustic Response

The basic physical structure of the broadband underwater acoustic response, under the specific condition that the essential features of the states of all acoustic scatterers, are known is first presented in order to provide intuition for the modeling that will follows where the state of scatterers, their acoustic ranges and instantaneous speeds are not known. For notational simplicity this development is limited to pressure fields that are cylindrically symmetric, only propagation paths in the vertical plane encompassing source and receiver are specified. Each acoustic path linking source and receiver exhibits geometric spreading and frequency dependent volume attenuation [16] [28]. Let l_{mxt} represent the m^{th} acoustic path length at time t and receiver location x. Let $\tau_{mt} = \int_{l_{mx_ot}} d\mathbf{s}/c(st)$ be the propagation delay to a reference element on the array. Further let $\theta_{m,t}$ represent its arrival angle at the array so that the wave vector is $\bar{k}_m = \omega(\hat{r}cos\theta_m + \hat{z}sin\theta_m)/c_o$. The amplitude and phase contribution at radian frequency ω of the acoustic pressure field at the receiver array element at location x due to this m^{th} eigen-path is therefore

$$h_{mx\omega t} = l_{mt}^{-1+\epsilon_m} e^{-\alpha_\omega l_{mt} + \sum_k \gamma_{mp}(\omega)} e^{-j(\omega\tau_{mot} + \bar{k}_{mt}\cdot\bar{x}_t)}. \quad (1)$$

The first term captures attenuation due to geometric spreading with $|\epsilon_m|$ summarizing the along path refractive effects through the volume. The second term summarizes the volume attenuation due to sea-water absorption losses [16] [28]. The term $\sum_p \gamma_{m,p}(\omega)$ summarizes the boundary interactions where $\text{Re}\{\gamma\}$[nepers], $\text{Im}\{\gamma\}$[radians]. Here $\gamma_{m,p}$ is the reflection coefficient of the p^{th} boundary interaction along the m^{th} acoustic path. The final term captures the aggregate phase rotation associated with propagation over the acoustic path to each of the elements of the array where x is the position of the x^{th} array element relative to the reference element location. Significant time variations in the response function are due to the time dependent path delay time and the time dependent angle of incidence at the receiver. The aggregate acoustic response function is the superposition of the M arrivals,

$$h_{x\omega t} = \sum_m^M h_{mx\omega t}. \quad (2)$$

The inverse Fourier transform of this response with respect to ω is the impulse response function between source and receiver at location-time xt, Consider a receive aperture of D equally spaced elements located at $x_d = d\Delta_z\hat{z}, d = [0, .D-1]$ relative to our reference. The response function in the directions associated with $\sin(\phi_k) = [0 : D-1]/D$ are

$$h_{k\tau t} = \textstyle\sum_d h_{d\tau t} e^{-j\omega \sin(\phi_k)\Delta_z d/c_o}. \quad (3)$$

The Fourier transform with respect to propagation delay is

$$2\pi h_{k\omega t} = \textstyle\int h_{k\tau t} e^{-j\omega\tau}\, d\tau, \quad (4)$$

providing the amplitude and phase response over the channel bandwidth at geo-time t, The Fourier transform over geo-time is

$$2\pi h_{k\omega\nu} = \textstyle\int h_{k\omega t} e^{-j\nu t}\, dt, \quad 2\pi h_{k\tau\nu} = \int h_{k\tau t} e^{-j\nu t}\, dt. \quad (5)$$

provides the Doppler bandwidth of the delay path processes. Here notation is simplified by retaining h as the response function regardless of the bases over which it is defined. Let the indices denote the Fourier transform such that $U_{k\omega\nu}$ operates on h as

$$h_{k\omega\nu} = U_{k\omega\nu} h_{d\tau t} \quad (6)$$

A communication receiver must employ a model of the channel spread and dynamics in order to estimate and track channel changes such that energy from the arrivals can be combined. For this purpose we present a hierarchical Gaussian mixture model of channel spreading.

B. A Gaussian mixture model over beam frequency and Doppler

Underwater acoustic response functions can vary greatly across ocean environments as well as over time in a given ocean environment. Certain bottom materials and roughness, water sound speed and surface wave spectra imply statistical constraints on the acoustic response functions and these can vary greatly both spatially and temporally. The acoustic receiver algorithm must be robust to spatial and temporally varying channel conditions with limited or no prior information regarding any of the acoustic environment parameters. For the practical case where the arrival amplitudes, delay times and angles are not known exactly we make a few assumptions to simplify the model. To this end consider two classes of arrivals. The first are those arrivals with relatively few boundary interactions such that their phase processes $\omega\tau_m(t)$ are relatively narrow band relative to some fixed bandwidth of $\Delta_\nu << W$, where W is the source signal bandwidth. The superposition of these arrivals with unknown amplitudes and phases can be considered as well approximated by a complex Gaussian distribution at any given frequency ω. Likewise the arrivals that have Doppler bandwidth that exceeds the symboling duration W/N_s where N_s is the processing gain of the symboling design. These paths are rapidly time varying and have a phase processes that appears white like when sampled at the period N_s.

Conditioned on a relative speed between source and receiver platforms with range rate of v_o the mean Doppler is known and the distribution of the acoustic response function we therefore will be modeled by the following hierarchical model

$$\begin{aligned}\pi_{k\nu\omega}|v_o, \pi_k &\sim \pi_k D(\nu - v_o\omega/c_o)S(\omega)\\ z_{k\nu\omega}|\pi_{k\nu\omega} &\sim Ber(\pi_{k\nu\omega}),\\ h_{k\nu\omega}|z_{k\nu\omega} &\sim N_{h_{k\nu\omega}}^{z_{k\nu\omega}}(0,\lambda_{k\omega}^2) \times N_{h_{k\nu\omega}}^{1-z_{k\nu\omega}}(0,\epsilon_k^2).\end{aligned} \tag{7}$$

The factor π_k is the a priori probability of ensonifying the k^{th} beam. The factor D is a marginal or average Doppler spectrum and captures the prior likelihood of the channel paths' scatterers possessing a given aggregate velocity $v \propto c_o \times \nu/\omega$. This average Doppler spectrum has the interpretation of a probability density function. The model captures coherent energy at beam Doppler frequency slot $k\nu\omega$ through the indicator variable $z_{k\nu\omega} = 1$ and the model specifies that channel energy at $k\nu\omega$ is incoherent if $z_{k\nu\omega} = 0$. The model is useful primarily because it allows for the parsimonious treatment of sparse time varying arrivals and the analytic solution of all posterior moments leading to computationally reasonable solutions. It thereby provides a useful adaptive structure for estimation of the acoustic response from observations. It is noticed that the model provides for a broadband Doppler model with Doppler offset dependent on frequency.

C. Posterior inference for acoustic response function

Assume that the symbols exhibit orthogonality over the multi-path delay band, i.e. $C_{\mathbf{b}}$ the convolution operator associated with the sent symbols satisfies $C_{\mathbf{b}}'C_{\mathbf{b}} = I$. Let $\mathbf{r}$ represent the array data over the symboling interval. It follows that the posterior density of the acoustic Green's function [9] [10] over the symboling epoch is

$$\begin{aligned}p(\mathbf{h}|\mathbf{r},\mathbf{b}v_o) &\propto N_{\mathbf{r_d}}(C_{\mathbf{b}}\underbrace{U_{k\omega\nu}^{-1}\mathbf{h}}_{\mathbf{h}_{d\tau t}}, I) \times\\ &\prod_{k\omega\nu}\left(\pi_{k\omega\nu}N_{h_{k\omega\nu}}(0,\lambda_{k\omega}^2) + (1-\pi_{k\omega nu})N_{h_{k\omega\nu}}(0,\epsilon_k^2)\right).\end{aligned} \tag{8}$$

leading to

$$\begin{aligned}p(\mathbf{h}|\mathbf{r},\mathbf{b}) \propto \prod_{k\omega\nu}(&\pi_{\check{h}_{k\omega\nu}}N_{h_{k\omega\nu}}(\gamma(\lambda_{k\omega})\check{h}_{k\omega\nu}, \gamma(\lambda_{k\omega})) +\\ &(1-\pi_{\check{h}_{k\omega\nu}})N_{h_{k\omega\nu}}(\gamma(\epsilon_k)\check{h}_{k\omega\nu}, \gamma(\epsilon_k)))\end{aligned} \tag{9}$$

where the least squares estimates are

$$\check{\mathbf{h}}_{k\omega\nu} = U_{k\omega\nu}\check{\mathbf{h}}_{d\tau t} \quad , \quad \check{\mathbf{h}}_{d\tau t} = C_{\mathbf{b}}'\mathbf{r}$$

and

$$\begin{aligned}\pi_{\check{h}_{k\omega\nu}}^{-1} &= 1 + \frac{1-\pi_{k\omega\nu}}{\pi_{k\omega\nu}}\frac{N_{\check{h}_{k\omega\nu}}(0,\epsilon_k^2+1)}{N_{\check{h}_{k\omega\nu}}(0,\lambda_{k\omega}^2+1)}\\ \gamma(x) &= x^2/x^2+1\ .\end{aligned}$$

Since mixture Gaussian priors are conjugate for Gaussian likelihood functions the posterior density (9) is also a mixture Gaussian. The posterior mean is a weighted average of each model's average and since the posterior model probabilities $\pi|\mathbf{r}$ are also functions of the data the result, while akin to a classic Wiener filter, has an additional adaptable feature in the mixture weights. The result is an empirical Bayes (EB) shrinkage operator of the raw $k\omega\nu$ measurements $\check{\mathbf{h}}_{k\tau\nu}$,

$$E[h_{k\omega\nu}|\mathbf{r},\mathbf{b},\hat{\epsilon},\hat{\lambda}] = \left(\pi_{\check{h}_{k\omega\nu}}\gamma(\lambda_{k\omega}) + (1-\pi_{\check{h}_{k\omega\nu}})\gamma(\epsilon_k)\right)\check{h}_{k\omega\nu}$$

and letting S denote the EB soft shrinkage rule

$$\hat{\mathbf{h}}_{k\omega\nu} = S_{\check{\mathbf{h}}}(\check{\mathbf{h}}_{k\omega\nu}). \tag{10}$$

This EB posterior expectation greatly attenuates smaller, noise-like coefficients while leaving the larger coefficients unchanged. The γ's are Wiener-like gains over each delay-Doppler element. The EB estimate of variance is

$$\begin{aligned}\hat{\upsilon}_{k\omega\nu} &= var[h_{k\omega\nu}|\mathbf{r},\mathbf{b},\hat{\epsilon},\hat{\lambda}]\\ &= \left(\pi_{\check{h}_{k\omega\nu}}\gamma(\lambda_{k\omega}) + (1-\pi_{\check{h}_{k\omega\nu}})\gamma(\epsilon_k)\right)\\ &+\pi_{\check{h}_{k\omega\nu}}(1-\pi_{\check{h}_{k\omega\nu}})(\gamma(\lambda_{k\omega\nu})-\gamma(\epsilon_k))^2 \times \check{h}_{k\omega\nu}^2\end{aligned} \tag{11}$$

and can be understood as $\mathrm{var}[h_{k\omega\nu}] = E_{z_{k\omega\nu}}\mathrm{var}[h_{k\omega\nu}|z_{k\omega\nu}] + \mathrm{var}_{z_{k\omega\nu}}E[h_{k\omega\nu}|z_{k\omega\nu}]$. The parameters $\{\lambda_{k\omega}, \epsilon_k, \pi_{k\omega\nu}\}$ allow for adaptation of the model to the observations and they, like the gains, are estimated from the data, see for instance [9] [10]. An EB Laplace approximation to the posterior distribution of the acoustic response function in the phone-delay-time domain is therefore

$$\begin{aligned}p(\mathbf{h}_{d\tau t}|\mathbf{r},\mathbf{b},\hat{\epsilon},\hat{\lambda}) &\approx N_{\mathbf{h}}(U_{d\tau t}\hat{\mathbf{h}}_{k\omega\nu}, U_{d\tau t}\Upsilon U_{d\tau t}')\\ \Upsilon &= \mathrm{Diag}(\hat{\upsilon}).\end{aligned} \tag{12}$$

III. Estimation of aggregate path dilation

One critical advantage of accurate coherent estimates of the acoustic response function is that the bulk dilation process associated with the acoustic arrival delay times can be estimated and factored out of the Green's function by "un-dilating" the received acoustic waveform. These path delay time processes are driven largely by source receiver motion in the case of mobile communicators but also by common ocean volume forces. For many underwater acoustic applications platform velocity is relatively minimal in the vertical direction as vehicles typically transit at a constant depth. For small acoustic angle spreads in shallow water range rate is the dominant factor in the shared delay time processes. For this reason arrival time variations for horizontally moving platforms are correlated having common time varying components. These facts account for the efficacy of phase tracking algorithms and the phase locked loop [21] for mobile communications in multipath channels and underwater acoustic communications [24] in particular. Here the acoustic response function is used to capture all delay-Doppler behavior over the signaling epoch up to the resolution of the symbol duration and the aggregate arrival time variations are then deduced from this estimate. The bulk path dilation estimate defines a natural time-varying sampling rate for the acoustic response that nearly "straightens out" or compensates for the shared time variation of the acoustic paths. The remaining time variations of the acoustic arrivals constitute the natural coherence time of the ocean acoustic response function. The Doppler bandwidth $1/2N_sW$ associated with the symbol interval determines the bandwidth of the final estimate and this is set by the processing gain and signaling bandwidth. For instance at a bandwidth of 20 kHz and a processing gain of 1000 the observable Doppler bandwidth is 20 Hz. Consider the two cases: 1) A time invariant shared dilation rate, the shared component of the delays is a simple linear function of time. 2) Time-varying dilation, allowing for a common, shared temporal variation in the acoustic arrival times over the symboling interval. These two are considered and suitable estimators are presented.

A. Time invariant path dilation rate

Factoring out a common linear delay drift, consider the model of the M dimensional arrival process as

$$\tau_{dm}(t) = \delta_o t + \delta\tau_m(t) \ \ , \ m = \{1, \dots M\} \tag{13}$$

where δ_o is a shared dilation rate among all of the paths. The following estimate of the mean dilation rate over all paths and over the duration of the message is [10]

$$\hat{\delta_o} = \frac{1}{D}\sum_d \int \frac{\nu}{\omega} \frac{|\hat{h}_{d\omega\nu}|^2}{\int |\hat{h}_{d\zeta\xi}|^2 d\zeta d\xi} d\nu d\omega. \tag{14}$$

B. Time-varying path dilation rate

Factoring out a common time varying delay process, the model of the M dimensional arrival process is

$$\tau_{dm}(t) = \delta_o(t) + \delta\tau_m(t) \ \ , \ m = \{1, \dots M\} \tag{15}$$

where $\delta_o(t)$ is a shared dilation process among all of the paths. Using a Laplace approximation of the density of the channel [10] the following estimate of the mean dilation rate over all paths and over the duration of the message is

$$\hat{\delta_o}(t) = \omega_c^{-1} \frac{1}{D}\sum_d arg\left[\int |\hat{h}_{d\tau t}|^2 \cdot e^{j\angle \hat{h}_{d\tau t} - \angle \hat{h}_{d\tau 0}} d\tau\right]. \tag{16}$$

This estimator weighs the phase rotation rate at each delay in proportion to it's energy so that the dominant arrivals dominate the estimate.

IV. An M-ary orthogonal signaling for underwater acoustic communications

The signaling scheme that is used to test these proposed adaptive filtering schemes is similar to that of the M-ary Walsh/m-sequence signaling tested by Iltis [14]. Performance bounds have been derived for M-ary orthogonal spread spectrum signaling through fading channels for the case of independent channel gains [23] [2] [6] [7] [20] and specific algorithms for diversity combining of M-ary orthogonal signals have been explored [27]. In this present study it is assumed that the symbol sets have good orthogonal properties over the multipath spread of the acoustic channel. The essential feature of such an M-ary signal set is that the symbol sequences $\mathbf{c}_m$, $m = 1, ...M$, obey

$$C_k' C_l = I \times \delta_{k-l} + E_{k,l} \tag{17}$$

where C_m is the convolution operator associated with the code word $\mathbf{c}_m$. The matrix E has all coefficients less than $1/N_s$ where N_s is the sequence length. The receiver estimates the sent bit stream in the following iterative manner,

$$\begin{aligned} \hat{\mathbf{h}}^i &= E_{h|b=\hat{b}}[\mathbf{h}|\mathbf{r}, \mathbf{b} = \hat{\mathbf{b}}^{i-1}, \tau_o = \hat{\delta_o}^{i-1}] \\ \hat{\mathbf{b}}^i &= \arg\max_{\mathbf{b}} p(\mathbf{b}|\mathbf{r}, \mathbf{h} = \hat{\mathbf{h}}^i, \delta_o = \hat{\delta_o}^i) \\ \hat{\delta_o}^i &= \arg\max_{\tau_o} p(\mathbf{h}_{\tau_o}|\mathbf{r}, \mathbf{b} = \hat{\mathbf{b}}^{i-1}). \end{aligned} \tag{18}$$

Here, as previously, $\mathbf{h}$ represents the double spread channel function, $\mathbf{b}$ represents the sent bit stream of interest and δ_o represents the aggregate time varying dilation rate. Iterative receiver structures can now be constructed from any of the various conditional estimators of channel and dilation rate coupled to symbol decisions conditioned on those estimates. In this section a few such receivers that provide a good compromise between accuracy and computational cost are discussed. Coherent and non-coherent symbol decisions are considered but only of the hard decision type.

A. Symbol decision rules

In this channel estimation based scheme symbol decisions are made conditioned on the data $\mathbf{r}$ and the channel parameter estimates which of course are functions of the data. For simplicity we ignore the variance of the channel estimates in the decision process. The likelihood function for each symbol is of the form

$$\mathbf{r}_t|\mathbf{h}_t, b_t \sim N_{\mathbf{r}}(C_{b_t}\mathbf{h}_t, I) \qquad b_t \in \{1, 2 \dots M\}$$

where b_t specifies the sent codeword at the t^{th} symboling frame determining the $N_s + L - 1 \times L$ convolution operator C_{b_t}.

B. Coherent soft and hard decisions

With equally probable and equal energy symbols the probability of $b = m \in$ and ignoring the variance of the channel function estimation errors approximate as $P(b = m|\mathbf{r}, \mathbf{h} = \hat{\mathbf{h}}) = p(\mathbf{r}|b = m, \mathbf{h}) / \sum_{m'} p(\mathbf{r}|b = m', \mathbf{h} = \hat{\mathbf{h}})$. The results is

$$P(b_t = m|\mathbf{r}, \mathbf{h}) \approx \frac{e^{2Re[\hat{\mathbf{h}}' C_m' \mathbf{r}_t]}}{\sum_l e^{2Re[\hat{\mathbf{h}}' C_l' \mathbf{r}_t]}} \tag{19}$$

and approximate ML decisions conditioned on the channel iteration estimate are

$$\hat{b}_t \approx \arg\max_m \quad Re[\hat{\mathbf{h}}_t' C_m' \mathbf{r}_t] \quad (\mathrm{WPC-C}). \tag{20}$$

We denote this symbol decision rule as weighted path combining with coherent decisions (WPC-C).

C. Noncoherent soft and hard decisions

Likewise non-coherent symbol estimates and decisions are based on $|\hat{\mathbf{h}}' C'_m \mathbf{r}_t|^2$. Assume perfect orthogonality of the symbol code words over the L lag delay band $C_m C_{m'} = I_L \delta_{m-m'}$ and for simplicity in what follows define $\tilde{\mathbf{h}} = \mathbf{h}/|\mathbf{h}|^2$ and noting that the M statistically independent $\tilde{\mathbf{h}}' C'_k \mathbf{r}_t$ complex scalar variables are Gaussian distributed

$$\begin{aligned} \tilde{\mathbf{h}}'_t C'_m \mathbf{r}_t | b_t = m &\sim N_x(|\mathbf{h}|_2, 1), \\ \tilde{\mathbf{h}}'_t C'_m \mathbf{r}_t | b_t \neq m &\sim N_x(0, 1) \end{aligned}$$

so that

$$\begin{aligned} x_m^2 = |\tilde{\mathbf{h}}' C'_m \mathbf{r}_t|^2 &\sim \chi_2^2(|\mathbf{h}|_2^2) \ , \\ x_{k|m}^2 = |\tilde{\mathbf{h}}' C'_k \mathbf{r}_t|^2 &\sim \chi_2^2 \end{aligned} \tag{21}$$

where $\chi_2^2(\lambda^2)$ represents a non-central chi-square random variable [17] with non-centrality parameter λ^2 and $\chi_2^2 = \chi_2^2(0)$ is the standard central chi-square random variable. Let $p_{\chi_2^2(\lambda)}(x)$ denote the density function of a non-central chi-square random variable with non-centrality parameter λ. It follows that symbol probabilities can be approximated by conditioning on the estimated channel response. It follows that $P(b_t = m | x_1^2, \ldots, x_M^2), \mathbf{h} = \hat{\mathbf{h}}) = p(\mathbf{r}|b = m, \mathbf{h}) / \sum_{m'} p(\mathbf{r}|b = m', \mathbf{h} = \hat{\mathbf{h}})$ and therefore

$$P(b_t = m | \mathbf{r}, \mathbf{h}) \approx \frac{p_{\chi_2^2(|\hat{\mathbf{h}}|^2)}(|\tilde{\mathbf{h}}' C'_m \mathbf{r}_t|^2)}{\sum_{k \in \mathcal{M}} p_{\chi_2^2(|\hat{\mathbf{h}}|^2)}(|\tilde{\mathbf{h}}' C'_k \mathbf{r}_t|^2)} \ . \tag{22}$$

Hard decisions are simply

$$\hat{b}_t = \arg\max_m \ |\hat{\mathbf{h}}'_t C'_m \mathbf{r}_t|^2 \ (\mathrm{WPC-NC}). \tag{23}$$

Denote this symbol decision rule as weighted path combining with non-coherent decision (WPC-NC).

V. Results.

An M-ary orthogonal spread spectrum receiver structure has been demonstrated to provide coherent combining through multi-path and Doppler spread channels. The proposed iterative receiver structures were tested on M-ary orthogonal spread spectrum experimental data taken in Buzzard's Bay MA in June of 2009. Probability of bit error over a range of SNRs were computed by Monte-Carlo averaging of the receiver's error rate statistics. Presented here are comparisons of coherent and non-coherent symbol decisions with coherent channel estimation and time varying Doppler compensation. The receivers tested are listed and described in Table I. Rough synchronization and Doppler estimation are derived from short (1 symbol duration) broad band synchronization signals that initialize the algorithm. For all cases tested the received signal to noise ratio (rSNR) is measured as the in-band signal power average to the whitened noise power average over the entire signaling packet. Spreading gains are such that throughput rates for these schemes are as follows: 4-ary corresponds to approximately 95 bps while 8-ary corresponds 131 bps.

Figure 1 displays the WHOI-09 experiment location and the particular placement of source and receiver platforms. Two receivers, one approximatley 1km from the Tioga source and the other approximately 2km. The water is approximately 20m deep and the bottom is of a gravel type. The source and receiver transducers are roughly mid water column and the water is approximately isovelocity. The center frequency of the experiment was 32kHz and the bandwidth was approximately 20kHz.

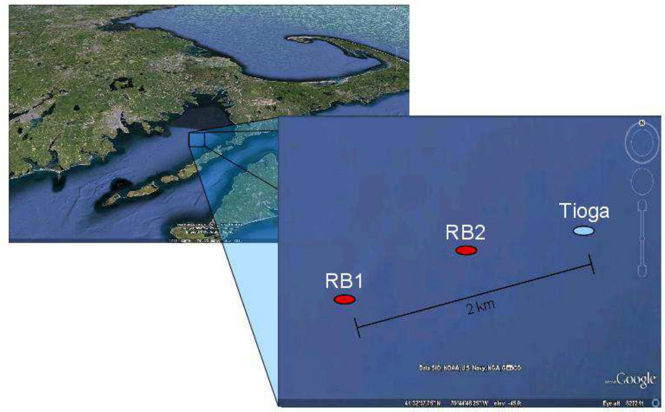

Fig. 1. Location of the Buzzard's Bay Massachusetts experiment in the summer of 2009. RB2 is the location of a receiver buoy at 1km from the source at the vessel Tioga. RB1 is the location of a receiver buoy at 2km from the source.

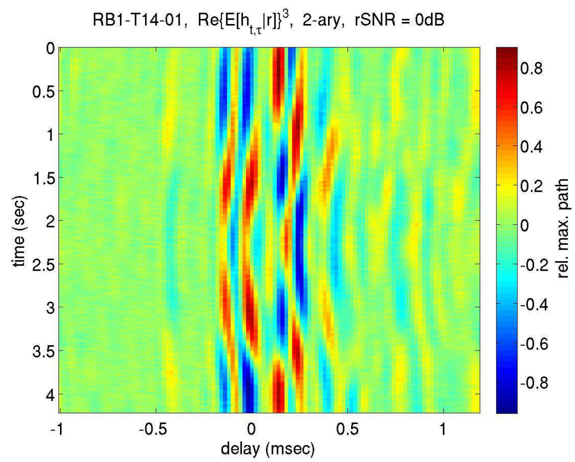

Fig. 2. Real part of estimated impulse response function at 0 dB SNR from 2 km at RB1 from a 2-ary orthogonal spread spectrum message with 3 element combining.

To illustrate the value of the proposed scheme as a means to focus coherent acoustic energy dispersed in Doppler bandwidth by source-receiver motion consider a few examples of the proposed receiver's dilation compensation method. Figure 2 and Figure 3 presents an example at 0 dB received SNR of an acoustic Green's function before and after time varying dilation compensation. In both cases the results are taken from a joint symbol and channel estimation procedure associated with an acoustic communications signal. The first is after one iteration after initial channel and symbol estimates while Figure 3 is that of the third iteration following time varying Doppler compensation.

Figure 4 and Figure 5 presents an example of the efficacy of

TABLE I. ITERATIVE RECEIVER ALGORITHMS FOR M-ARY ORTHOGONAL SPREAD SPECTRUM SIGNALING

Receiver 1		
WPC-non-coh. decisions with symbol-aided time-invariant timing estimation		
Parameter	Initialization	Iterative estimator
symbol decision $\mathbf{b}^i$	$p(\mathbf{b}^0) = M^{-K}$ or	Eq. (23)
acoustic response: $\mathbf{h}^i$	Eq. (10)	Eq. (10)
bulk path dilation: δ^i	Eq. (14)	Eq. (14)
resampling operator:	N/A	[10]
three symbol decision iterations total		
Receiver 2		
WPC w/ coh. decisions with symbol-aided time-varying timing estimation		
Parameter	Initialization	Iterative estimator
symbol decision: $\mathbf{b}^i$	$p(\mathbf{b}^0) = M^{-K}$ or	Eq. (20)
acoustic response: $\mathbf{h}^i$	Eq. (10)	Eq. (10)
bulk path dilation: $\delta^i(t)$	Eq. (14)	Eq. (16)
resampling operator:	N/A	[10]
three symbol decision iterations total		

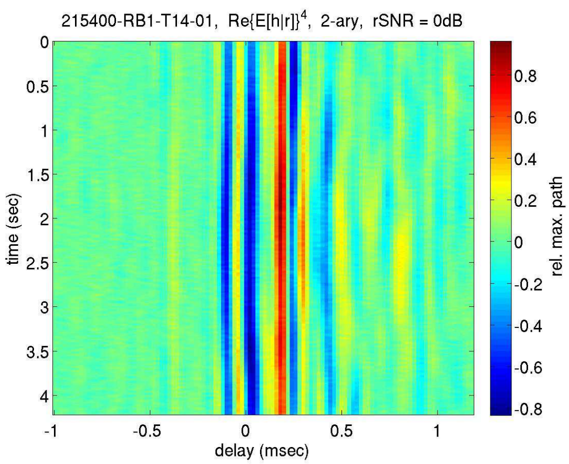

Fig. 3. Real part of estimated impulse response function after timve varying dilation compensation at 0 dB SNR from 2 km at RB1 from a 2-ary orthogonal spread spectrum message with 3 element combining

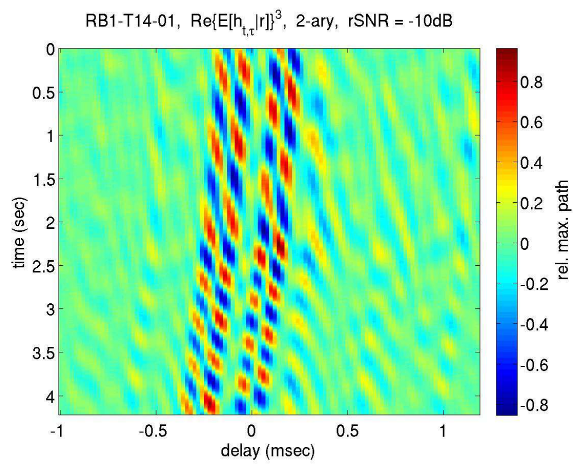

Fig. 4. Real part of estimated impulse response function at -10 dB SNR from 2 km at RB1 from a 2-ary orthogonal spread spectrum message with 3 element combining.

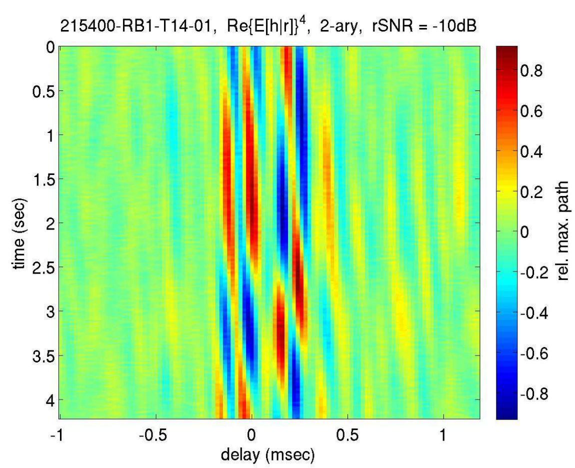

Fig. 5. Real part of estimated impulse response function after time varying dilation compensation at -10 dB SNR from 2 km from a 2-ary orthogonal spread spectrum message with 3 element combining.

the channel and dilation process estimation and compensation at -10 dB received SNR.

Consider now the performance in terms of bit error rate for the proposed receiver algorithm at a range of SNRs. Figure 6 gives bit error rate results as a function of SNR where performance ranges from a probability of bit error of 10^{-1} to about 10^{-6}. The propagation range is 2 km, the bandwidth is 20kHz for a throughput rate is 95 bps. It is noticed that with 3 element combining bit error rates are well under 10^{-4} at an SNR/bit of 11 dB corresponding to -13 dB received SNR. The difference between non-coherent and coherent symbol decisions is approximately 2 dB across apertures.

Figure 7 gives bit error rates for the receiver over a range of SNRs. The propagation range is again 2 km. The spreading gain is such that at 20 kHz bandwidth the throughput rate is 95 bps. It is noticed that with 3 element combining bit error rates are well under 10^{-4} at an SNR/bit of 9 dB corresponding to -18 dB received SNR. The difference between non-coherent and coherent symbol decisions is again approximately 2 dB across apertures.

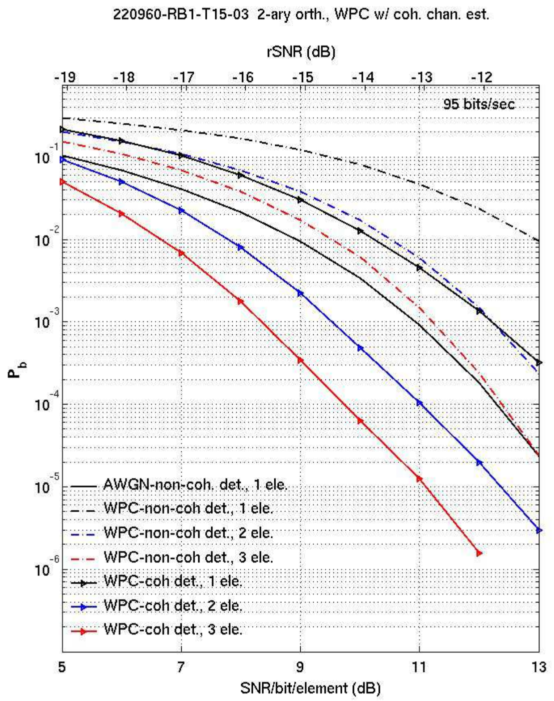

Fig. 6. Performance of 2-ary orthogonal spread spectrum signaling at 2km in 20 meters of water.

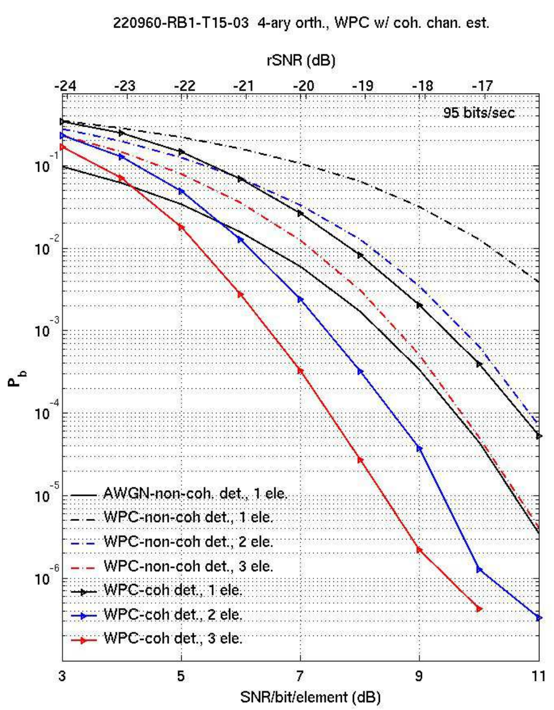

Fig. 7. Performance of 4-ary orthogonal spread spectrum signaling at 2km in 20 meters of water.

Figure 8 gives bit error rate results for a wide spread of

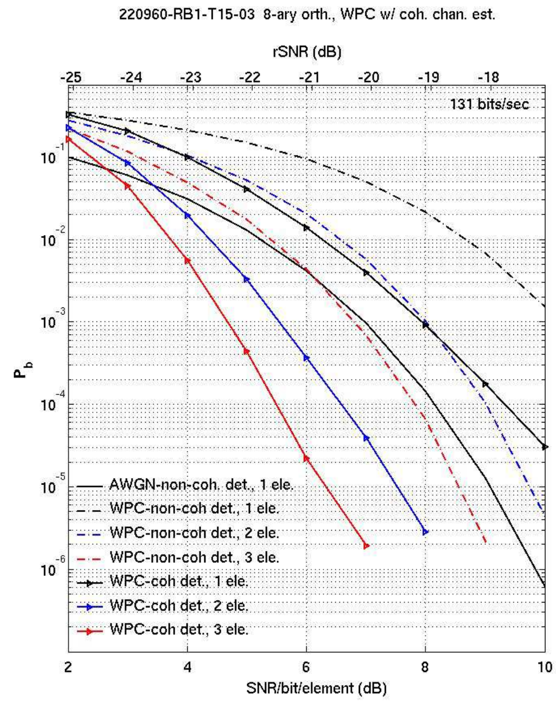

Fig. 8. Performance of 8-ary -orthogonal spread spectrum signaling at 2km in 20 meters of water.

SNRs where bit error rates range from 10^{-1} to about 10^{-6}. The propagation range is 2 km. The throughput rate is 131 bps. It is noticed that with 3 element combining bit error rates are well under 10^{-4} at an SNR/bit of 6 dB corresponding to -21 dB received SNR. The difference between non-coherent and coherent symbol decisions is approximately 2 dB across apertures.

VI. Conclusion

A means of coherent channel estimation in doubly spread shallow water acoustic channels is provided to support communication at very low SNR. The scheme has been tested in at-sea trials with implementations employing both coherent and non-coherent symbol decisions. The schemes are well suited for low rate, very low SNR underwater acoustic communications and are presented as a means to extend the range and duration of acoustic surveillance assets. These signal processing methods can be adapted to multi-user communications and MIMO applications.

Acknowledgment

These M-ary orthogonal signaling schemes were tested at-sea by Lee Freitag who planned and executed the WHOI-09 acoustic communication experiments.

References

[1] H. Kopka and P. W. Daly, *A Guide to LaTeX*, 3rd ed. Harlow, England: Addison-Wesley, 1999.

[2] V. Aalo, O. Ugweje, R. Sudhakar, “Performance analysis Analysis of DS/CDMA systems with noncoherent M-ary orthogonal modulation in Nakagami fading” *IEEE Trans. on Vehicular Technologies, Vol. 47, June 1999, pp 111-117.*

[3] Teledyne-Benthos, “Product Catalog 2010, Wireless Subsea Communications” *http://www.benthos.com/pdf/*

[4] P.J. Crepeau, “Asymptotic performance of M-ary orthogonal modulation in generalized fading channels” *IEEE Trans. Commun., Vol 36, No 11, November 1988, pp 1246-1249...*

[5] P. Dahl, et al., “Underwater Ambient Noise” *Acoustics Today*, Vol 3 Issue 1 pp 23-33. January 2007.

[6] A. Dekorsy, K.D. Kammeyer M-ary Orthogonal Modulation for Multi-Carrier Spread-Spectrum Uplink Transmission Proceedings of IEEE International Conference on Communications (ICC), Vol. 2 (June 1998), pp. 1004-1008.

[7] A. Dekorsy, S. Fischer, K. Kammeyer, Maximum likelihood decoding of M-ary orthogonal modulated signals for multi-carrier spread-spectrum systems Personal, Indoor and Mobile Radio Communications, 1998. The Ninth IEEE International Symposium on Boston MA, 8-11 Sep 1998, page(s): 538 - 543 vol.2, ISBN: 0-7803-4872-9 INSPEC Accession Number: 6275687, Digital Object Identifier: 10.1109/PIMRC.1998.734261

[8] L. Freitag, M. Johnson, M. Grund, S. Singh, and J. Preisig, “Integrated Acoustic Communications and Navigation for Multiple UUVs” *Proc. Oceans 2001* Honolulu, HI, pp 2065-2070 (2001).

[9] P.J. Gendron, “An Empirical Bayes estimator for in-scale adaptive filtering” *IEEE Transactions on Signal Processing,* Vol. 56, No. 5, pp 1670-1683, May 2005.

[10] P.J. Gendron, “Sparse Broadband Acoustic Response Estimation via a Gaussian Mixture Model with Application to M-ary Orthogonal Signaling” *Canadian Acoustics, Special on Marine Acoustics* Vol. 40, No. 1, pp 39-53, March 2012.

[11] D. Green, “Acoustic Modems, navigation aids and networks for undersea operations” *IEEE OCEANS 2010 Conference*, Sydney Aus, May 2010,

[12] L. Freitag, M. Stojanovic, S. Singh, M. Johnson, “Analysis of channel effects on direct sequence and frequency-hopped spread-spectrum acoustic communications” *IEEE Journal of Ocean Engineering*, Vol. 26, (4) pp 586-593, 2001.

[13] S. Haykin, “Adaptive Filter Theory”, Prentice Hall Information and System Sciences Series, New Jersey, 2002.

[14] R. J. Iltis, “A Sparse Kalman Filter with Applicaiton to Acoustic Communications Channel Estimation” *IEEE/MTS OCEANS 2006*, ISBN 1-4244-0114-3, 18-21 September 2006.

[15] W. Jakes, “Microwave Mobile Communications”, 1^{st} *Edition IEEE Press* 445 Hoes Lane, Piscataway, NJ, 1993,

[16] F.B. Jensen, W.A. Kuperman, M.B. Porter, H.Schmidt “Computational Ocean Acoustics”, *AIP Press, AIP Series in Modern Acoustics and Signal Processing* ISBN 1-56396-209-8

[17] N.L. Johnson, S. Kotz, “Distributions in Statistics: Continuous univariate distributions-2,” *John Wiley* & *Sons, Wiley Series in Probability and Mathematical Statistics, 1970.* ISBN 0-471-44627-0.

[18] H. Kermorgant, “Architecture of AUV systems for harbour protection and mine countermeasure” *Oceans 2005 Europe*, Vol. 2, pp 1400-1405, June, 2005.

[19] I.F. Alyildiz, D. Pompili, T. Moldia, “Underwater acoustic sensor networks: research challenges” *Ad Hoc Networks, (Elsevier)*. Vol. 3. no. 3. pp 257-279, May 2005.

[20] I.D. Panagiotis, F-N. Pavlidou, DS/CDMA M-ary orthogonal signaling in shadowed Rayleigh channel for mobile communications, Wireless Networks, Vol. 2, pp 343-357.

[21] J. Proakis “Digital Communications”, *McGraw-Hill, Inc.*, 1221 Avenue of the Americas, New York, NY 10020, 2000.

[22] J. S. Sadowsky, V. Kafedziski, “On the Correlation and Scattering Functions of the WSSUS Channel for Mobile Communications”, *IEEE Transactions on Vehicular Technology* Vol. 47, No. 1, February 1998.

[23] M.K. Simon, M.S. Alouini, “Bit error probability of noncoherent M-ary orthogonal modulation over generalized fading channels.” *Int. J. Commun. and Networks, Vol 1, No 2. February 1998, pp 20-29.*

[24] M. Stojanovic, “Multichannel detection for wideband underwater acoustic CDMA communications” *Journal of Oceanic Engineering, 2006, Vol 31 No. 3 pp 685-695*.

[25] R. Stokey, L. Freitag, M. Grund, “A compact control language for AUV acoustic communications” *IEEE/OES Oceans Europe 2005*. Vol. 2, pp 1133-1137, 20-23 June 2005

[26] R. Stokey, et al., “Very shallow water mine countermeasures using the REMUS AUV: a practical approach yielding accurate results” *IEEE/MTS OCEANS 2001*. Vol. 1, pp 149-156, 2001.

[27] J.S. Thompson, P.M. Grant, B. Mulgrew, “Algorithms for coherent diversity combining of M-ary orthogonal signals” *IEEE Journal on Selected Areas in Communications*, Vol 17, Issue 11, November 1999, pp 1886-1899.

[28] R. J. Urick, “Principles of Underwater Sound 3rd Edition” *Peninsual Publisher, 1996*. ISBN-13: 978-0932146625.